Response to Reviewer 2's Comments

Dear reviewer,

We sincerely thank you for your careful reading of our manuscript and for your constructive and insightful comments. We greatly appreciate your recognition of the potential value of the dataset and the proposed VSRE index, as well as your important concerns regarding the scope of ESSD, the conceptual basis of VSRE, the rationale for the validation design, and the overall organization and presentation of the manuscript.

In response to these comments, we have substantially revised the manuscript to make its data-descriptor focus clearer and to improve its logical structure, methodological transparency, and readability. Most importantly, we have clarified that the primary contribution of this study is the ChinaTidalVSC dataset, a spatially continuous 10 m vegetation structural complexity product for China's tidal wetlands, rather than the development of a general-purpose methodological framework. Accordingly, VSRE is now presented more explicitly as a necessary data-generation and standardization procedure for converting UAV-LiDAR point clouds into an ecologically interpretable and reusable structural-complexity variable.

We have also strengthened the explanation of the experimental and ecological basis for the low-, medium-, and high-complexity groups, and clarified that the biomass-weighted Shannon index was used as an independent ecological proxy associated with community structural differentiation, rather than as a direct ground truth of vegetation structural complexity. In addition, we have reorganized the Methods and Results sections to better follow the logic of a data-description article, added a central workflow figure, improved the description of LiDAR data acquisition and processing, clarified the distinction between fixed-plot validation and nationwide field samples, and reframed the comparisons with existing metrics as data validation and quality assessment rather than broad methodological benchmarking.

To further improve the reusability of the dataset, we have added clearer guidance on potential applications, data format, value interpretation, and limitations. We have also expanded the data repository from a single GeoTIFF file to a more complete data package, including metadata, sample-level information, validation data, and VSRE calculation code where appropriate. We have revised the title, Abstract, Introduction, Methods, figure captions, and Data availability section accordingly, and have checked the manuscript for terminology consistency and typographical errors.

We believe that these revisions have substantially improved the focus, rigor, transparency, and accessibility of the manuscript. We hope that the revised version more clearly demonstrates the suitability of this work as an ESSD data-description article and provides sufficient information for users to understand, evaluate, and reuse the ChinaTidalVSC dataset.

Below, we provide a detailed point-by-point response to each comment. (*Black Italic*: *reviewer comments*; Blue: our responses; Purple: revised text).

Comment 1: *Coastal wetlands fulfil important ecosystem services such as carbon sequestration, shoreline protection and water purification. Since these services depend on vegetation structure, quantifying structural complexity of coastal wetlands allows estimating and predict ecosystem service provision. The manuscript introduces a new LiDAR-based vegetation structural complexity (VSC) index called Vegetation Structural Relative Entropy (VSRE) and presents a VSRE map for the coast of China. The authors state that the existing VSC metrics are not tailored to coastal wetlands, which differ from forest ecosystems for which these metrics have been typically developed.The authors introduce the VSRE and compute it for LiDAR data of coastal wetlands across the coast of China. Based on Alpha Earth Foundation data, they further use an MLP deep learning model to produce a VSRE map for the entire coast of China (for 2022). They compare how both the VSRE and five other VSC metrics capture different levels of VSC or biodiversity and different plant communities, and how robust they are to varying point densities.*

Response: We are very grateful for your recognition of the value of our research. Your encouraging comments on the clarity, organization, and contribution of our study are highly appreciated, and they motivate us to refine our work further.

Comment 2: *The dataset is interesting, and the index could be very valuable. However, after reading the manuscript, many aspects are still not clear to me. Most importantly, I am not sure if the manuscript in its current form fits the scope of ESSD.ESSD states that "manuscripts that focus on methodology and model development should seek publication elsewhere", that "extensive analysis and interpretation of data is considered out of scope" and that "any comparison to other methods is beyond the scope of regular articles". Since the manuscript introduces a new method/index and has quite substantial analysis in the form of comparison to other metrics (and a lot of Supplementary Data), I feel like the focus of the paper does not match a data description article.*

Response: We thank the reviewer for raising this important concern regarding the scope of ESSD. We understand that the manuscript may appear, at first sight, to have a strong methodological component because it introduces VSRE and compares it with existing vegetation structural complexity metrics. However, we would like to clarify that the primary aim of this manuscript is to describe and publish a new, quality-controlled, wall-to-wall dataset of vegetation structural complexity for China's tidal wetlands.

The central data product of this study is ChinaTidalVSC, a 10 m spatially continuous dataset designed to be directly usable by researchers in ecology, remote sensing, coastal science, and Earth system modelling. To generate such a dataset, it was necessary to convert raw UAV LiDAR observations into a standardized, ecologically interpretable structural-complexity variable. In this sense, VSRE serves as a data-generation and data-standardization procedure, rather than as the final purpose of the manuscript. This is consistent with the ESSD scope, which allows articles to describe nontrivial methods used to filter, normalize, or convert raw observations into primary published data.

We agree that ESSD regular articles should avoid extensive interpretation of data and broad methodological comparisons. Our intention in comparing VSRE with existing VSC metrics was not to conduct a comprehensive method-development study or to claim a general replacement of existing metrics across all ecosystems. Instead, these comparisons were included as essential quality assessment and fitness-for-use tests for the published dataset. Because the proposed dataset is intended for broad reuse by ecologists and Earth scientists, users need to know whether the derived VSC values are sensitive to known structural gradients, robust to varying LiDAR point-cloud densities, and suitable for low-stature and heterogeneous coastal wetland vegetation. Therefore, the comparisons with conventional horizontal, vertical, and integrated structural metrics were used only to demonstrate the reliability, robustness, and ecological validity of the published data product.

We also note that the statistical analyses used in these comparisons are standard and limited in scope. They provide the minimum necessary evidence that the raw LiDAR data were appropriately transformed into a robust, reusable VSC dataset. Similarly, the figures and supplementary analyses are intended to document parameter selection, algorithm stability, model performance, and uncertainty, which are important components of data description and quality control.

Nevertheless, we recognize that the current organization of the manuscript may have unintentionally overemphasized the methodological aspects. In the revised manuscript, we will further clarify the data-descriptor nature of the paper and adjust the presentation accordingly.

Specifically, we will:

1. revise the Abstract and Introduction to state more explicitly that the main contribution is the ChinaTidalVSC dataset, rather than the development of a general VSC method;

2. clarify in the Methods that VSRE is used as a necessary procedure to convert raw LiDAR point clouds into the primary published dataset;

3. reframe the comparisons with existing metrics as data validation and quality assessment.

4. reduce or reorganize interpretive statements in the Results and Discussion to avoid overextending beyond the scope of a data description article; and

5. move some technical details and supporting comparisons to the Supplementary Materials where appropriate.

We hope that these revisions will make the manuscript's scope clearer.

Our goal is to provide a transparent, well-validated, and reusable dataset for the scientific community, together with sufficient methodological documentation to ensure that users can understand how the data were generated, evaluate their reliability, and apply them appropriately in future coastal wetland studies.

Comment 3: *The dataset is a single tiff file with the VSRE map. Since there is no "usage" section, it is not clear how other researchers benefit the dataset. For which studies could it be used?*

Response: We thank the reviewer for this constructive suggestion. We will add a dedicated "Usage" section to explain how ChinaTidalVSC can be used by other researchers.

ChinaTidalVSC provides a continuous, 10 m spatially explicit measure of vegetation structural complexity across China's tidal wetlands. Unlike categorical vegetation maps or optical vegetation indices, this dataset captures within-type and within-region structural heterogeneity, which is often difficult to detect from vegetation classification products alone. Therefore, the dataset can be used as a structural covariate in studies of coastal ecosystem services, blue carbon modelling, shoreline protection, habitat quality assessment, biodiversity and conservation prioritization, restoration planning, and the validation or benchmarking of future remote-sensing products of coastal vegetation structure.

In response to this comment, we will revise the manuscript to include clearer guidance on potential applications, data format, value scaling, recommended preprocessing steps, and important limitations. We will also update the Figshare repository description to include this information so that users can correctly interpret and reuse the dataset.

Revised text:

Usage of data in Figshare

ChinaTidalVSC is designed as a reusable spatial dataset for ecological, remote-sensing, and coastal-zone studies that require quantitative information on vegetation structural complexity (VSC). The dataset provides a wall-to-wall 10 m map of vegetation structure relative entropy (VSRE) for coastal China in 2022. Because VSRE is a continuous structural variable, it provides information beyond vegetation presence/absence, vegetation type, or optical greenness indices.

Potential applications include the following:

1. **Coastal ecosystem service assessment**

ChinaTidalVSC can be used as a structural covariate to assess ecosystem services that depend on vegetation architecture, such as wave attenuation, shoreline protection, sediment trapping, habitat provision, and resistance to physical disturbance. Areas with higher structural complexity may indicate more heterogeneous vegetation architecture and potentially stronger functional capacity, although the relationship should be evaluated for each specific service.

2. **Blue carbon and coastal biogeochemical modelling**

Vegetation structure can influence productivity, litter input, sediment capture, and soil organic carbon accumulation. ChinaTidalVSC can therefore be incorporated into blue carbon models or spatial carbon assessments as an additional predictor of ecosystem structure, especially where vegetation classification alone is insufficient to represent functional differences among or within plant communities.

3. **Habitat quality and biodiversity studies**

Structural complexity is widely recognized as an important component of habitat heterogeneity. This dataset can support studies that examine the relationship between coastal vegetation structure and biodiversity, including birds, benthic fauna, insects, or other wetland-dependent organisms. It may also help identify structurally complex habitat patches within the same vegetation type.

4. **Conservation prioritization and restoration planning**

ChinaTidalVSC can help identify coastal wetland areas with high structural heterogeneity or regions where vegetation structure is relatively simplified. These patterns may be useful for prioritizing conservation areas, evaluating restoration outcomes, selecting reference sites, or identifying locations where vegetation recovery has not yet translated into structural recovery.

5. **Comparison with vegetation classification and optical indices**

The dataset can be used together with vegetation-type maps, EVI, NDVI, or other optical indices to distinguish compositional and structural dimensions of coastal wetlands. For example, two areas classified as the same vegetation type may have different VSRE values, indicating different internal structural conditions.

6. **Remote-sensing product validation and benchmarking**

ChinaTidalVSC can serve as a reference dataset for developing, validating, or benchmarking future remote-sensing products of coastal vegetation structure, especially products derived from optical imagery, SAR, spaceborne LiDAR, UAV data, or multimodal foundation-model embeddings.

7. **Spatial heterogeneity and regional comparison**

The dataset enables users to quantify structural variation within estuaries, nature reserves, restoration zones, administrative regions, or coastal biogeographic units. Summary statistics such as mean, median, variance, and quantiles of VSRE can be calculated for user-defined regions to compare structural conditions across space.

Recommended use:

Users should first mask the raster to their study area or coastal wetland boundary of interest. Because the stored raster values are scaled integers, the original VSRE value should be obtained by dividing the stored value by 10. For example, a stored raster value of 235 corresponds to a VSRE value of 23.5. Pixels marked as NoData in the raster metadata should be excluded from analysis. When aggregating VSRE to larger spatial units, we recommend reporting not only the mean value but also the median, standard deviation, and quantiles, because structural complexity can be highly heterogeneous within coastal wetlands.

Important considerations:

ChinaTidalVSC represents vegetation structural complexity for the year 2022 and should not be interpreted as a long-term average or as a direct measure of temporal change. The dataset quantifies vegetation structural heterogeneity rather than vegetation species composition, biomass, carbon stock, or ecosystem service supply itself. Therefore, when used for ecological interpretation, it should ideally be combined with vegetation maps, field observations, environmental covariates, or process-based models. In addition, although the dataset was generated and validated using LiDAR-derived VSRE samples and Alpha Earth Foundation embeddings, uncertainties may remain in areas with sparse training data, highly dynamic tidal conditions, fragmented vegetation patches, or mixed land-water pixels.

Comment 4: *Furthermore, it would be extremely valuable to the scientific community if the UAV-LiDAR data and ideally also the field data would be included in the dataset.*

Response: We thank the reviewer for this valuable suggestion. We agree that the scientific value and reusability of the dataset would be substantially improved if more supporting data were provided in addition to the wall-to-wall VSRE map.

In response, we will expand the data repository from a single GeoTIFF file to a more complete and reusable data package. In addition to the 2022 wall-to-wall VSRE GeoTIFF, the revised repository will include: (i) a README and metadata file describing file names, projection, spatial resolution, units, valid value ranges, NoData values, value scaling, and recommended usage; (ii) the coastal tidal-wetland mask used for mapping; (iii) sample-level metadata for the 1,337 field LiDAR samples, including sample ID, geographic location, vegetation type, point-cloud density, acquisition year, quality-control flags, and LiDAR-derived VSRE values; (iv) vector files representing the sample footprints or centre points of the field LiDAR samples; (v) validation data used for map evaluation; and (vi) the VSRE calculation code.

We also agree that making the UAV-LiDAR and field data available would be highly valuable. However, the complete original flight-scale UAV-LiDAR point clouds are very large, contain substantial information beyond the purpose of the present VSRE map, and require additional point-cloud-specific quality control, documentation, and metadata before they can be responsibly released as a standalone dataset. Moreover, these raw point clouds have broader potential applications beyond the scope of this data-description article, including vegetation classification, terrain modelling, biomass estimation, and coastal geomorphological analysis. Therefore, the present manuscript focuses on the derived vegetation structural complexity product and the sample-level information required to interpret, evaluate, and reuse this product.

To improve transparency and reproducibility, we will provide reviewer access to the expanded data package through an anonymous repository review link during revision. Upon final publication, the data package will be released publicly with a persistent DOI. We will revise the Data availability section accordingly to clarify which data are included in the public repository, which data are provided for review, and how users may access additional LiDAR or field data for collaborative or extended analyses.

Comment 5: *How were these three qualitative VSC groups classified (cf. L80f.)? I could not find this in the paper (other than "human-defined complexity classification" in L390). Given that VSC is difficult to measure directly (as already stated by Reviewer 1), I think it is absolutely crucial for the manuscript and interpretation of the results and figures to explain this.*

Response:

We thank the reviewer for this important comment. We apologize for not explaining the basis of the three qualitative VSC groups clearly enough in the original manuscript. We agree that, because VSC is difficult to measure directly, the grouping criteria used for evaluating structural metrics must be explicitly defined and independently justified. We want to clarify that the low-, medium-, and high-VSC groups in this study were not defined solely by subjective human-visual assessment. Instead, they were derived from three representative coastal wetland community structure scenarios formed within a controlled near-natural experimental fixed plot and were further supported by independent field survey data.

Specifically, the experimental fixed plots used in this study were not natural plots selected at random, but were designed to represent three typical coastal wetland community-structure scenarios (**Fig. 1, 2**). The first scenario was a monodominant herbaceous community commonly associated with high salinity and high tide-level conditions, represented by the globally widespread *Phragmites australis* community. The second scenario was a mixed herbaceous community under medium-salinity and low-tide-level conditions. The third scenario was a mixed herbaceous--woody community under low-salinity and high-land with drier habitat conditions, which is more commonly observed in mangrove--saltmarsh ecotones.

In terms of ecological and structural characteristics, these three scenarios broadly correspond to an increasing complexity gradient under nearly-natural conditions, from monodominant saltmarsh vegetation to mixed herbaceous communities and then to herbaceous--woody assemblages. More importantly, these communities were not artificially planted or assembled. Instead, they developed through near-natural succession after ground-water levels above the water table (to simulate tide level) were regulated in this experimental platform, which has been operating since 2018. Besides, six replicate plots were established for each scenario to improve sample representativeness and reproducibility. Therefore, the structural gradient represented by these three plot groups was primarily defined by the experimental design and community formation processes, rather than by post hoc subjective visual assessment.

To further verify the objectivity of this structural gradient, we conducted herbaceous vegetation surveys and individual-tree segmentation during the same period as the LiDAR data collection (**Fig. S3,** 2025), and we quantified biomass and diversity across all sub-plots. Using these data, we constructed a biomass-weighted Shannon index based on each species' biomass proportion. This index served as an independent, continuous ecological proxy to examine whether the three subplot groups exhibited a significant structural complexity gradient. Rather than using individual abundances, as is common in many diversity calculations, we used each species' total biomass. This choice was necessary because herbaceous plants and woody trees often differ greatly in individual abundance, yet such numerical differences do not imply proportional differences in their contributions to spatial structural complexity. By contrast, biomass provides a common currency across growth forms and better reflects the relative contribution of different species to community structure, making it more appropriate for coastal wetland communities with large trait contrasts among plant growth forms. We further clarify that the Shannon index was not introduced here as a direct ground truth of VSC. Rather, in this experimental system, it provides a relatively bottom-up and objective structural reference at the level of community composition. As community biomass composition shifts from dominance by a single species to a more diverse assemblage, and from purely herbaceous vegetation to herbaceous--woody communities, the types and relative configurations of structural elements within the community generally increase in parallel. This pattern is consistent with our field observations of vegetation complexity in the sample plots (**Fig. 2**). Therefore, we consider this index an independent external proxy supporting the existence of a structural gradient, rather than a repeated expression of the metric being tested.

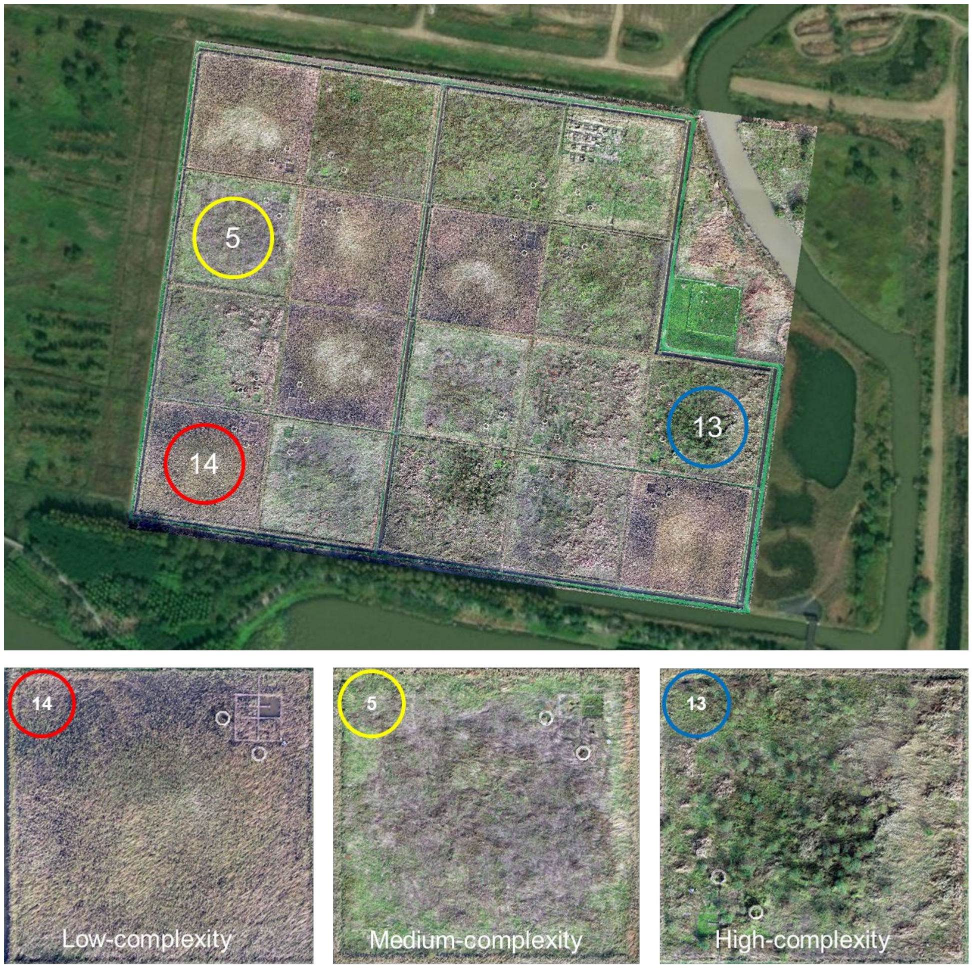

Fig 2. A high-resolution optical image of the fixed plot acquired in March 2025, with a spatial resolution of 0.5 cm pixel^{-1}.

The relevant results are shown in Fig. S3, which indicates a clear, consistent relationship between the human-observed and quantified gradients across the three subplot groups. We acknowledge that this supplementary figure was not explicitly cross-referenced in the main text, which made the basis of the grouping insufficiently clear. In the revised manuscript, we will add this explanation and explicitly state that Fig. S3 does not use the Shannon index as a direct ground truth of VSC. Instead, it uses an independent external proxy to support the rationale for the structural gradient represented by the three plot groups.

We also fully recognize that VSC in natural ecosystems does not always occur as discrete groups. More commonly, it varies continuously and may involve subtle structural differences. Therefore, we further introduced a continuous-gradient test in **Section 1.3.3**. In this analysis, the biomass-weighted Shannon index was used as a continuous external reference to test whether VSRE could respond to subplots without obvious categorical groupings but with gradual differences in VSC. The results showed that VSRE not only distinguished the three predefined structural scenarios but also maintained high sensitivity and stability along a continuous complexity gradient. This analysis complements the discrete-group comparison: the group-based test evaluates the discriminatory ability of the metrics in representative structural scenarios, whereas the continuous-gradient test further shows that VSRE is not effective only for strongly differentiated groups but can also detect more subtle structural variation that commonly occurs in natural ecosystems.

Based on these considerations, we believe that the three subplot groups used in this study have clear ecological representativeness, experimental reproducibility, and independent external support. They therefore provide a reasonable gradient system for evaluating the discriminatory ability of VSRE and other structural metrics in coastal wetland settings. In addition, the continuous-gradient analysis in **Section 1.3.3** further supports the effectiveness of VSRE in detecting more subtle structural variation closer to real ecological conditions.

Revised figures:

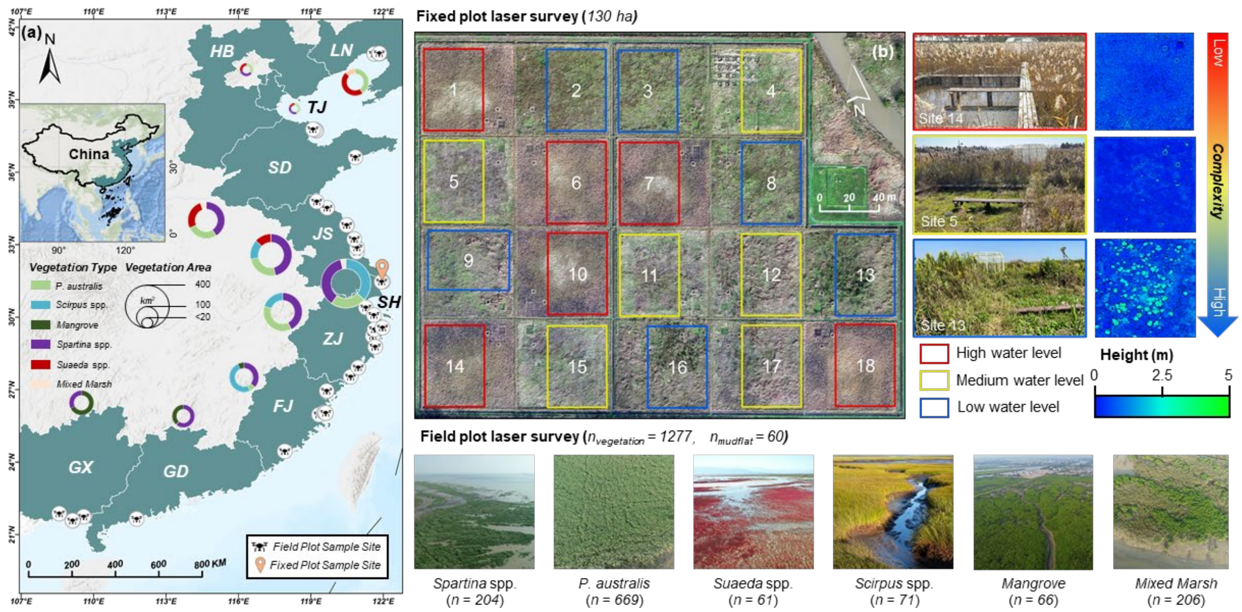

Fig. 1 | Overview of fixed plots and spatial layout of field drone sampling sites. a, Spatial distribution of all LiDAR sampling locations. Blue-green shading indicates sampled provinces, abbreviated with two-letter codes; drone icons represent the field LiDAR sampling sites, and the orange icon indicates the location of the fixed sampling site. **b**, LiDAR sampling conditions within fixed plots and primary vegetation communities surveyed. The LiDAR acquisition ranges under varying water levels are illustrated using three-color boxes, indicating that VSC decreases significantly as tidal levels rise. Representative field photos and digital surface elevation profiles from three sampling points are displayed on the right. Field-collected LiDAR data encompass six typical coastal wetland vegetation types, including succulent herbs (*Suaeda* spp., *Scirpus* spp.), graminoid vegetation (*Phragmites australis*, *Spartina* spp.), mixed marsh communities, and tree-dominated communities (mangroves).

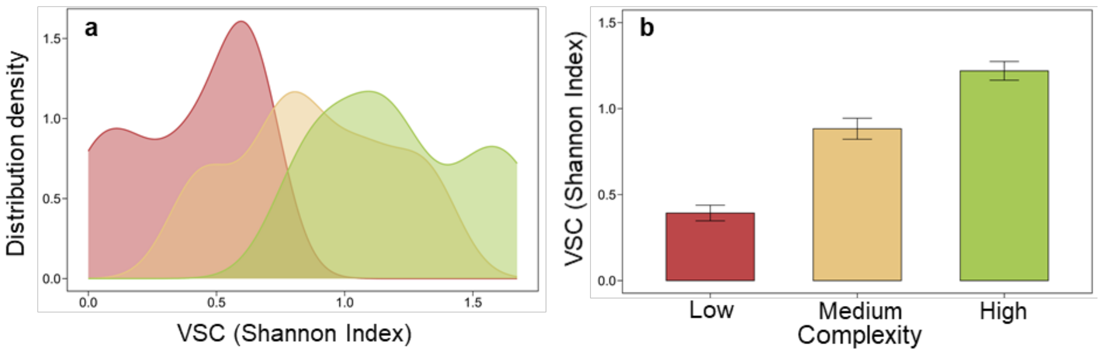

Fig. S3 | VSC index distribution characteristics constructed based on the Shannon index. a, the VSC distribution curve was fitted using kernel density estimation. **b,** Mean values of VSC in groups with different human-defined complexity. Error bars indicate standard deviation.

Comment 6: *You state that you use the Shannon Diversity Index as a "quantitatively objective VSC" (L391), but this index quantifies the diversity in terms of biomass but not in terms of structure, right? Please better explain the rationale here.*

Response: Response: We thank the reviewer for this important clarification. We agree that the Shannon diversity index, even when calculated using biomass proportions, does not directly quantify three-dimensional vegetation structure. It measures the evenness of biomass distribution among species, rather than the spatial arrangement, height distribution, or configurational heterogeneity of vegetation elements.

Our rationale was more specific to the experimental system used in this study. We used the biomass-weighted Shannon index as an independent continuous ecological proxy associated with community structural differentiation. Although biomass itself is not equivalent to structural complexity, it represents an important material basis for the formation of three-dimensional vegetation structure. A more even distribution of biomass among species or growth forms usually indicates that structural material is not dominated by a single morphological unit, but is more likely to be composed of vegetation elements differing in height, form, and spatial configuration. In this sense, biomass-weighted community heterogeneity can provide an external ecological gradient associated with structural differentiation, especially in a system where contrasting growth forms coexist.

This choice was also motivated by the specific characteristics of our fixed plots. The plots contained both herbaceous and woody plants, which differ greatly in individual abundance, body size, height, morphology, and contribution to spatial structure. If species richness or individual abundance were used directly, the extremely large number of herbaceous individuals could dominate the index and obscure the structural contribution of woody plants. By contrast, biomass provides a more comparable measure of the relative contribution of different species and growth forms to the material basis of vegetation structure. For example, a small number of woody individuals may contribute substantially to vertical and spatial structure, even though their numerical abundance is much lower than that of herbaceous plants.

Within our experimental platform, this biomass-weighted community gradient was consistent with several independent observations. The water-level treatments generated a transition from a monodominant herbaceous community, to a mixed herbaceous community, and then to a mixed herbaceous–woody community. This transition was accompanied by clear changes in field observations, community composition, plot photographs, and LiDAR-derived surface profiles. Therefore, in this specific experimental context, the biomass-weighted Shannon index provides a reasonable independent continuous ecological reference associated with increasing community structural differentiation.

Importantly, this analysis was not used as the sole or decisive evidence for the effectiveness of VSRE. Our evaluation framework included two complementary components. First, we compared VSRE and conventional structural metrics across the low-, medium-, and high-VSC groups generated by the water-level-controlled experimental platform. This group-based analysis tested whether different metrics could distinguish representative coastal wetland community-structure scenarios. Second, we used the biomass-weighted Shannon index as an independent continuous ecological reference to test whether different metrics could respond to gradual changes in community heterogeneity associated with structural differentiation. Thus, the continuous-gradient analysis was intended as a supplementary sensitivity test, rather than as a direct validation against ground-truth VSC.

In the revised manuscript, we will remove the phrase "quantitatively objective VSC" and replace it with more accurate wording, such as "an independent biomass-weighted community heterogeneity proxy associated with structural differentiation" or "a continuous ecological proxy related to community structural differentiation". We will also explicitly state that the biomass-weighted Shannon index quantifies biomass distribution among species and growth forms, not vegetation structure itself. This revision will make clear that the index provides supplementary ecological support for the experimentally generated structural gradient, rather than serving as a universal or direct ground truth of VSC.

Revised text and figures:

Because the initial VSC grouping of the secondary plots was based primarily on predefined vegetation community composition, structural characteristics, and expert field assessment, we further calculated a biomass-weighted Shannon diversity index as an independent and continuous reference for the degree of structural differentiation in each secondary plot. Biomass, rather than individual abundance, was used for weighting because the plots contained both herbaceous and woody plants, which differed markedly in individual abundance, body size, and contribution to three-dimensional spatial structure. Compared with diversity indices based on individual abundance, the biomass-weighted approach better reflects the relative contributions of different species and growth forms to the material basis of vegetation structure, thereby reducing bias introduced by the extremely high abundance of herbaceous individuals when characterizing community structure (Cousins, 1991).

Comment 7: *The manuscript would benefit from a central workflow figure. From the text alone, it is difficult to follow the steps you took to prepare the dataset.*

Response: Thank you for this helpful suggestion. We have revised the technical workflow figure to provide a more detailed and transparent illustration of the VSRE calculation process. The revised figure now includes the specific processing steps and procedures, thereby addressing the missing information in the original conceptual illustration.

Revised figure:

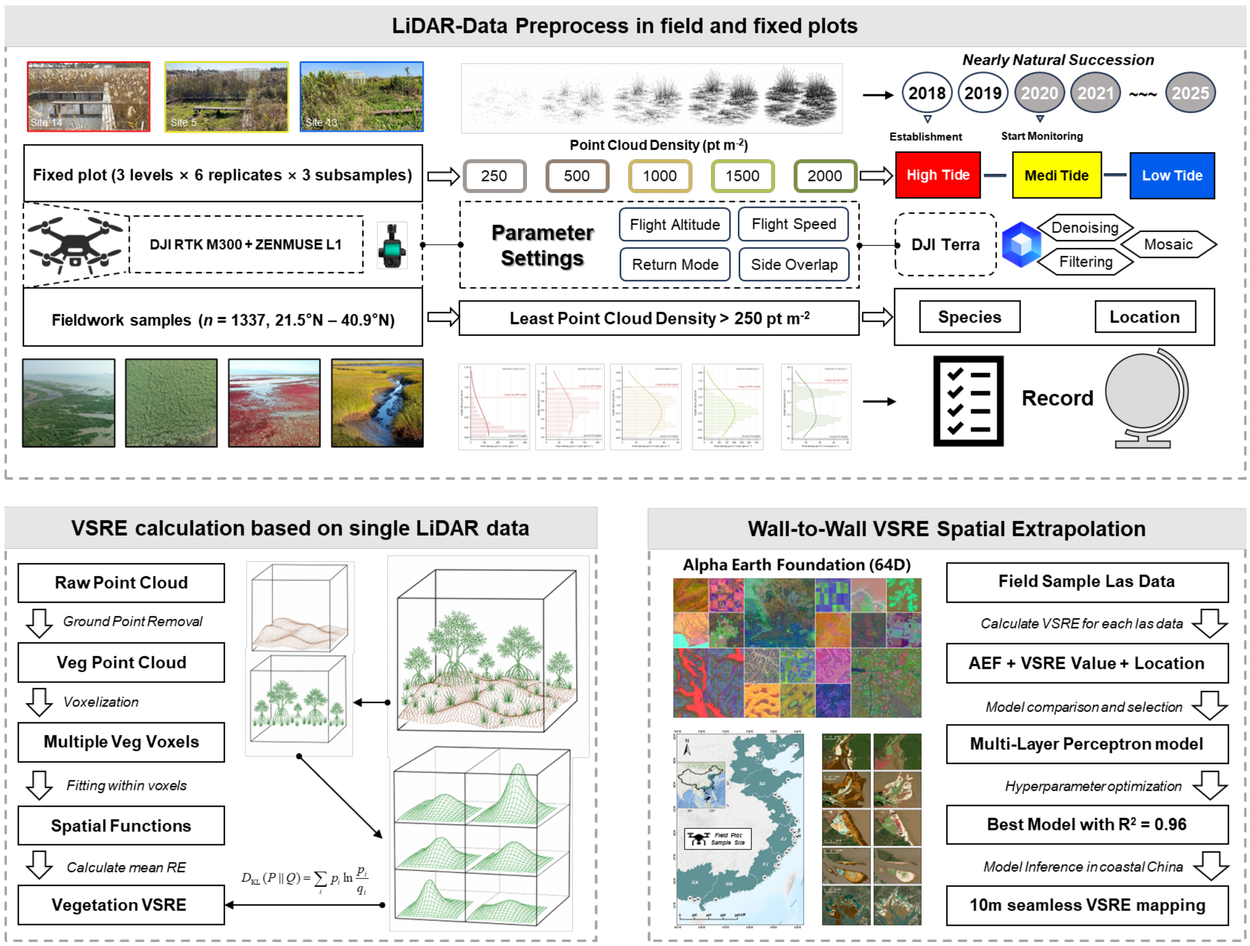

Fig. 3 | The Overall workflow of this study.

Comment 8: *Related to the previous point, the organization of the manuscript should be improved. Key information is difficult to find or overly vague and processing details are mentioned before an appropriate general overview is provided. Many data acquisition or processing steps remain unclear to me.*

Response: We thank the reviewer for this important suggestion. In the revised version, we will reorganize the Methods and Results sections following the logic of a data-description paper. We will first provide a general overview of the dataset, input data, workflow, and final outputs, and then describe the fixed-plot LiDAR data, nationwide field LiDAR samples, VSRE calculation, AEF-based mapping, and quality assessment in sequence.

We will also move overly detailed technical content that interrupts the narrative to the Supplementary Materials or Appendix, while retaining in the main text the information necessary for understanding and reproducing the dataset. These changes will make the manuscript easier to follow and help readers locate key data-acquisition and processing details more clearly.

Comment 9: *Is VSRE supposed to be a specific VI tailored for coastal wetlands or is it applicable to all kinds of vegetation ecosystems?*

Response: We thank the reviewer for raising this important question. We clarify that VSRE should not be interpreted as a universal vegetation index that can fully capture all dimensions of VSC across all vegetation ecosystems. In this study, VSRE was developed, parameterized, and validated primarily for coastal wetland vegetation.

Coastal wetland vegetation has several structural characteristics that differ from many terrestrial forest ecosystems: it is often low-stature, relatively open-canopied, spatially patchy, and composed of herbaceous and woody growth forms coexisting within a compressed vertical range. Under these conditions, local configurational heterogeneity is a particularly important dimension of vegetation structural complexity. VSRE was therefore designed to quantify differences among local three-dimensional point-cloud distributions, making it especially suitable for detecting structural heterogeneity in coastal wetland vegetation.

At the same time, the mathematical framework of VSRE is not inherently restricted to coastal wetlands. In principle, VSRE can be applied to other vegetation ecosystems if the input point clouds sufficiently capture the three-dimensional vegetation structure and if the parameters are adjusted according to the target ecosystem. These parameters include, for example, the vertical step size, maximum height, window size, and voxel settings. Therefore, VSRE can be viewed as a transferable analytical framework, but its parameterization and interpretation should be ecosystem-specific.

We also emphasize that VSRE primarily captures spatial configurational heterogeneity rather than total spatial occupancy. Therefore, in highly closed, structurally saturated forest ecosystems, VSRE alone may not represent all dimensions of VSC. In such cases, it should be used together with complementary metrics such as canopy cover, vegetation height, foliage height diversity, or spatial occupancy metrics.

In the revised manuscript, we will make this point clearer. We will describe VSRE as a VSC metric tailored for coastal wetlands and as a potentially transferable analytical framework.

Comment 10: *L86: In other locations in the manuscript, you state 1,337 sites, not 1,336? Also, are these 1,337 sites included in the acquisitions described in 1.2.1 or is this another dataset?*

Response: We thank the reviewer for carefully noting this inconsistency and for pointing out the ambiguity in our data description. The correct number is 1,337. The value “1,336” was a typographical error in the original manuscript, and we have corrected it throughout the revised manuscript.

We also clarify that the 1,337 samples are not the same dataset as the fixed experimental plots described in **Section 1.2.1**. In the revised manuscript, **Section 1.2.1** now specifically describes the fixed-plot LiDAR dataset collected from 18 secondary plots in the Dongtan water-level-controlled experimental platform. This dataset was mainly used for evaluating the performance and robustness of VSRE and conventional VSC metrics under controlled vegetation-structure gradients and different point-cloud densities.

In contrast, the 1,337 samples belong to the nationwide field LiDAR dataset now described separately in **Section 1.2.2**. These samples were extracted as 25 m × 25 m subsamples from 81 UAV-LiDAR scanning missions conducted along the mainland coast of China during 2022–2024. They were used to characterize natural coastal vegetation structural complexity across China and to support the wall-to-wall VSRE mapping.

To avoid further confusion, we have revised the manuscript structure by separating the fixed-plot LiDAR data and the nationwide field LiDAR data into two independent subsections. We also revised the overview figure and the relevant text in the Introduction and Methods to make their different sources and purposes clear.

Revised text and figures:

1.2.1 LiDAR data collection in the fixed plot

This study was based on the world's largest water-level-controlled wetland experimental plot, the Dongtan Ecosystem Experimental Plot (**121.94°E, 31.52°N**; Fig. 1). Established in 2018, this fixed plot has allowed vegetation to grow under natural coastal wetland conditions to date. The experimental setup includes three distinct water levels (-30 cm, 0 cm, and +30 cm), randomly distributed across a 130-hectare coastal wetland. The site was divided into 18 secondary plots, each measuring 60 × 60 meters, with two open-top chambers installed within each plot. Under these conditions, the vegetation communities developed distinct structural types: at the +30 cm tidal level, the community is dominated almost exclusively by *P. australis*; at the 0 cm level, diverse herbaceous species form mixed communities; and at the -30 cm level, mixed herbaceous species coexist with woody plants resembling mangrove structures. These naturally formed communities with contrasting vegetation structures provided ideal experimental conditions for our study.

We conducted LiDAR surveys over the fixed plot using a DJI Matrice 300 RTK drone equipped with a DJI Zenmuse L1 LiDAR sensor. Each flight mission covered the entire experimental site to ensure accurate spatial matching. For UAV acquisition, the return mode was set to 3 returns to improve the point cloud's ability to capture vegetation elements at different vertical positions. Point cloud densities were controlled by adjusting flight height and overlap rate, targeting approximate densities of 50, 100, 250, 500, 1000, 1500, and 2000 points m^{-2}. Datasets collected at 50 and 100 points m^{-2} were discarded due to excessive absorption by water surfaces (**Supplementary Fig 1**). Raw LiDAR data were processed in DJI Terra for stitching and denoising, and individual secondary plots were cropped to match the spatial extent of the ground survey plots. During cropping, we prioritized minimizing chamber inclusion while preserving all relevant vegetation features (specific cropping boundaries are shown in **Fig. 1b**).

1.2.2 LiDAR data collection in the field sites

We conducted extensive field surveys along the mainland coast of China from July to August, during the growing season of coastal vegetation, in 2022 and 2024. The surveys covered a latitudinal range from 21.5749°N to 40.9235°N (**Fig. 1a**). All surveys used the same UAV and LiDAR system, namely a DJI Matrice 300 RTK UAV equipped with a DJI Zenmuse L1 LiDAR sensor. A total of 81 LiDAR scanning missions, accompanied by synchronous optical photography, were conducted in major coastal vegetation hotspots. The LiDAR scans were acquired in three-return mode, and the expected point cloud density was maintained at >500 pt m^{-2} by adjusting flight altitude, flight speed, and side overlap. All data were collected under good visibility and low tide, when vegetation was fully exposed, to ensure simultaneous acquisition of high-quality optical imagery with a spatial resolution of approximately 0.5 m. These optical images supported subsequent accurate point-cloud cropping and vegetation type identification. In addition, we conducted 30 supplementary forest LiDAR surveys in Yunhe City, Zhejiang Province (**Supplementary table S1**), to compare potential differences in point-cloud structural characteristics across ecosystems and further assess the scalability of VSRE.

During data preprocessing, we further cropped the stitched raw point clouds. Based on vegetation patches and corresponding species information identified from high-resolution optical imagery, we extracted 1,337 25×25 m subsamples from the 81 stitched LiDAR datasets. Each subsample was associated with accurate latitude and longitude coordinates and vegetation type information, and adjacent subsamples were separated by at least 25 m. The point cloud density of the coastal vegetation subsamples ultimately ranged from 20.89 to 4,364.33 pt m^{-2}, with a mean value of 790.22 pt m^{-2}. The same cropping procedure was applied to the forest plots, but only one subsample was retained for each plot. The final point cloud density of the forest subsamples ranged from 142.04 to 1,271.73 points m^{-2}.

Comment 11: *Section 1.2.1: When was the data acquired? Did the flights use parallel flight strips, or, e.g., a criss-cross pattern? What was the flight speed? How did the overlap rates differ between flights? Please add more details?*

Response: We thank the reviewer for this helpful suggestion. We agree that the LiDAR acquisition procedure should be described in more detail, especially because the reliability of the derived VSRE values depends on the quality and consistency of the input point clouds.

In the revised manuscript, we will add more information on the acquisition period, UAV-LiDAR system, return mode, flight pattern, acquisition conditions, point-cloud density control, and preprocessing workflow. Specifically, we will clarify that the fixed-plot LiDAR data and the nationwide field LiDAR data were acquired during the vegetation growing season, and that the nationwide surveys were conducted from July to August in 2022–2024. All surveys used the same UAV-LiDAR system, namely a DJI Matrice 300 RTK UAV equipped with a DJI Zenmuse L1 LiDAR sensor. The LiDAR sensor was operated in three-return mode to improve the detection of vegetation elements at different vertical positions.

Regarding flight settings such as flight height, flight speed, and overlap rate, we clarify that these parameters were not used as independent analytical variables in this study. They were adjusted according to site-specific conditions, including vegetation height, terrain accessibility, flight safety, water coverage, and the required point-cloud density. Therefore, their exact values differed among missions and were mainly used operationally to achieve target point-cloud densities. For the purpose of VSRE calculation and data quality assessment, the more relevant and reproducible variable is the actual point-cloud density of each sample after processing, which we report in the manuscript and will include in the sample-level metadata.

For the fixed experimental plots, point-cloud density was intentionally controlled to produce multiple target density levels, including 50, 100, 250, 500, 1000, 1500, and 2000 points m^{-2}. The 50 and 100 points m^{-2} datasets were later excluded because water-surface absorption caused insufficient vegetation returns. For the nationwide field samples, flight parameters were adjusted in the field to maintain an expected point-cloud density greater than 500 points m^{-2} where possible. The final coastal vegetation subsamples had point-cloud densities ranging from 20.89 to 4,364.33 points m^{-2}, with a mean of 790.22 points m^{-2}. These actual point-cloud densities will be reported for each of the 1,337 samples in the public sample-level metadata.

We will also clarify that the raw point clouds were stitched and denoised in DJI Terra, and that individual fixed plots and nationwide 25 m × 25 m samples were then cropped from the processed point clouds. This revision will make the acquisition and preprocessing steps more transparent while avoiding overemphasis on mission-specific flight settings that were used only to achieve the required point-cloud density. The revised text can be found in the response to **comment 10**.

Comment 12: *L138: Which algorithm was used exactly for individual tree segmentation? Li et al. 2012? This part is very vague and should be explained better.*

Response: We thank the reviewer for pointing this out. We agree that the description of the individual-tree segmentation procedure was too vague in the original manuscript.

We clarify that individual trees were segmented using a canopy-height-model-based seed-point approach implemented in LiDAR360 (Morsdorf et al., 2004). Specifically, we first used the highest-density fixed-plot LiDAR dataset (2000 points m^{-2}) to generate a canopy height model (CHM) after terrain normalization. Local height maxima in the CHM were then detected as candidate tree-top seed points. These seed points were used to guide crown-object segmentation, and the resulting individual-tree objects were assigned to the corresponding secondary plots according to their spatial positions. This procedure follows the general logic of CHM-based individual-tree detection and crown segmentation, in which tree-top seeds are first identified and then used to delineate individual crown regions.

In the revised manuscript, we have described the individual-tree segmentation procedure more explicitly and cite the correct method paper.

Revised text and figures:

For woody plants growing in the center of the plots, considering the presence of sophisticated equipment monitoring soil respiration and vegetation carbon flux, we refrained from entering the plots for measurement to avoid interference and damage. Therefore, based on the highest point cloud density (2000 pt m^{-2}), we used a CHM-based individual-tree detection implemented in LiDAR360 software (Morsdorf et al., 2004), to segment individual trees within the fixed plots and assigned each segmented tree to its corresponding secondary plot (Fischer et al., 2019). The diameter at breast height (DBH) and crown height (CH) were recorded for each tree extracted using the segmentation algorithm. We measured the location, height, and DBH of 7 trees at the edge of the plots and compared them with vegetation parameters calculated after individual tree segmentation. The results showed that the errors were extremely small ($nRMSE_{CH}$ = 5.7%, $nRMSE_{DBH}$ = 2.4%). Furthermore, we identified tree species (mainly *Sapium sebiferum*) using UAV optical imagery and selected a matching allometric growth model to estimate biomass. Subsequently, we used a species-specific binary allometric growth model based on DBH and CH (Jucker et al., 2022) to calculate the total tree biomass of each secondary forest plot.

Comment 13: *L140f.: How was it possible to measure DBH from UAV-LiDAR data? Doesn't such data usually have too low point density for that? Or was DBH measured in the field? Please explain.*

Response: We thank the reviewer for pointing out this unclear description. We agree that DBH estimation from UAV-LiDAR data is often difficult, especially in closed-canopy forests or in datasets with low point density.

We clarify that DBH was estimated only for woody plants in the fixed experimental plots, and only using the highest-density LiDAR dataset with a target point-cloud density of 2000 points m^{-2}. It was not estimated from the nationwide field LiDAR samples or from lower-density point-cloud datasets. In our fixed plots, the woody plants were relatively low-stature, sparse, and open-canopied, and were mixed with herbaceous vegetation rather than forming a closed forest canopy. Under these conditions, the high-density UAV-LiDAR point cloud provided sufficient stem and lower-canopy returns to identify the woody stems and estimate stem diameter. This workflow has been proved effective in previous researches(Ye et al., 2025; Dalla Corte et al., 2020).

After CHM-based individual-tree segmentation, each segmented woody individual was assigned to its corresponding secondary plot. For each segmented tree, we used the terrain-normalized high-density point cloud to identify the stem region and estimate DBH from the point-cloud cross-section around breast height. To evaluate the reliability of this procedure, we also measured the location, height, and DBH of seven accessible trees at the edge of the plots in the field and compared these field measurements with the LiDAR-derived estimates. The comparison showed small errors, with nRMSE values of 5.7% for tree height and 2.4% for DBH. These field measurements were therefore used as an independent check of the LiDAR-derived tree parameters, but DBH was not field-measured for all trees in the fixed plots.

We will revise the manuscript to make this clearer. In particular, we will specify that DBH estimation was based on the highest-density fixed-plot point cloud, not on all UAV-LiDAR data.

Comment 14: *As someone who has not used allometric models yet, this part seems very vague. Can you add the equation for the allometric model?*

Response: Thank you for this helpful comment. We agree that the description of the woody biomass calculation was too vague in the original manuscript, especially for readers who are not familiar with allometric models.

We have revised the Methods section to explicitly provide the allometric equation used for estimating woody-plant biomass in the fixed plots(Walker et al., 2016). Because this biomass estimate was only used to calculate the biomass-weighted Shannon index as an independent VSC proxy, rather than to calculate VSRE itself, we used a published tree aboveground-biomass allometric equation based on DBH, tree height, and wood density (Tian, 2014):

$$\mathbf{AGB = 0.0017 + 0.294 \times D^2 \times H}$$

where (AGB) is the aboveground biomass of tree in kg, (D) is DBH in cm, and (H) is tree height in meter. DBH and tree height were derived from the highest-density fixed-plot LiDAR point cloud after individual-tree segmentation and were checked against field measurements for accessible trees. The biomass of all segmented trees was then summed within each secondary plot to obtain the plot-level woody biomass.

We further clarified that this allometric calculation was used only to estimate the woody-plant biomass component required for the biomass-weighted Shannon index in the fixed experimental plots.

Comment 15: *L181: What voxel size was used in this study and why?*

Response: Thank you for this helpful comment. We agree that the description of the voxel/window setting was not sufficiently clear in the original manuscript. In the VSRE calculation, we used a hierarchical spatial design rather than a single fixed voxel size. Specifically, a larger three-dimensional analysis box/window was first used to define the local structural unit, and this box was then discretized into smaller vertical voxel/bin units to construct normalized point-cloud probability distributions.

The size of the larger analysis box was selected to capture representative local vegetation structure while avoiding excessive mixing among different vegetation patches. In contrast, the vertical voxel/bin size was selected based on the minimum relevant vegetation height. Because coastal wetland vegetation includes low-stature herbaceous species, the vertical voxel/bin should be no larger than the minimum vegetation height; otherwise, low vegetation layers may be merged with the near-ground layer and subtle vertical structural differences would be lost. Therefore, we used 0.5 m as the vertical voxel/bin size, which corresponds to the lowest height scale of herbaceous marsh vegetation and was also the finest vertical resolution tested in our grid-search analysis.

We further clarify that the overall vertical range of the analysis box was adjusted according to the vegetation height range of each application. For the fixed-plot analysis, the maximum vertical calculation range was set to 5 m because the tallest plants in the plots were approximately 5 m. For the field coastal samples, which included taller mangrove communities, the maximum vertical calculation range was increased to 10 m, while the vertical voxel/bin size was kept at 0.5 m to retain sensitivity to low-stature saltmarsh vegetation. We have revised the ***Methods*** section to explicitly distinguish the larger analysis box from the smaller voxel/bin and to explain the rationale for these parameter settings.

Revised text and figures:

Revised main text 1:

Based on our field measurements, the tallest plants in our plots were trees at approximately 5 m, and the shortest were herbs at around 0.5 m; thus, we selected these as the maximum box height and Z-direction step size, respectively. Other hyperparameters were optimized using a grid search (**Supplementary Figures S1 and S2**).

Revised main text 2:

We applied the VSRE algorithm to 1,337 LiDAR samples collected from coastal regions of China. To accommodate the maximum potential height of mangroves in these areas (with 95% of individuals <10 m), we adjusted the maximum box height and Z-axis step size to 10 m and 0.5 m, respectively. Additionally, we modified the scaling constant to $1e^{-43}$ to expand the VSRE values into a more interpretable 0–100 range (***Methods***).

Comment 16: *L216ff.: These details on terrain normalisation seem to better fit into a different section.*

Response: Thank you for this helpful suggestion. We agree that the detailed description of terrain normalization interrupted the flow of the VSRE method section. Terrain normalization is a fundamental preprocessing step for LiDAR-based vegetation-structure analysis, because VSRE requires point heights to be expressed relative to the local ground surface rather than absolute elevation. However, the technical details of terrain fitting are not central to the conceptual description of VSRE. Therefore, we have moved the detailed terrain-normalization procedure, including the model formulation and equations, to the Supplementary Materials. In the main text, we now retain only a brief statement that all point clouds were terrain-normalized before constructing voxel-based probability distributions, with a cross-reference to the Supplementary Methods.

Revised text and figures:

Supplementary Methods: Line 164-195

To focus on structural diversity, the input point cloud data must first undergo terrain undulation removal. A Gaussian mixture model in the horizontal plane efficiently fits rugged terrain due to its multi-modal nature. Given a set of LiDAR point cloud data $\mathcal{P} = \{(\mathrm{x_I}, \mathrm{y_I}, \mathrm{z_i})\}_{\mathrm{i=1}}^{\mathrm{N}}$, where x_i, y_i, and z_i denote the 3D coordinates of the i^{th} point, the fitted surface $\hat{z} = f(x, y)$ can be expressed as (Wolfe, 1970):

$$\hat{z}(x, y) = \sum_{k=1}^{K} \omega_k \cdot G_k(x, y) \tag{S5}$$

Where $G(x, y) \sim \mathcal{N}(\vec{\mu}, \Sigma)$ is a bivariate Gaussian distribution. For the k^{th} distribution:

$$G_k(x, y) = A_k exp\left(-\frac{1}{2}\begin{bmatrix} x - \mu_k^{(x)} \\ y - \mu_k^{(y)} \end{bmatrix}^T \Sigma_k^{-1} \begin{bmatrix} x - \mu_k^{(x)} \\ y - \mu_k^{(y)} \end{bmatrix}\right) \tag{S6}$$

adopt learnable A_k as the amplitude, $\left(x - \mu_k^{(x)}, y - \mu_k^{(y)}\right)$ as the distribution center. Σ_k is the covariance matrix defining the distribution's orientation and spread:

$$\Sigma_k = \begin{bmatrix} {\sigma_k^{(x)}}^2 & \rho_k \sigma_k^{(x)} \sigma_k^{(y)} \\ \rho_k \sigma_k^{(x)} \sigma_k^{(y)} & {\sigma_k^{(y)}}^2 \end{bmatrix} \tag{S7}$$

Where ρ_k is the correlation coefficient and $\sigma_k^{(\cdot)}$ denotes the standard deviation in a given direction. To effectively fit real terrain, independent distributions with weights ω_k are linearly combined to form peaks ($\omega_k > 1$) or valleys ($\omega_k < 1$). The point cloud $\mathcal{P}$ is divided into grids (P × Q) along the x and y directions, extracting the minimum z-coordinate points in each grid as the ground morphology data S:

$$\mathrm{S} = \left\{\arg \min_{(x,y,z)\in\mathcal{P}} \mathrm{z} \mid (\mathrm{x}, \mathrm{y}) \in (\mathrm{x_p}, \mathrm{x_{p+1}}] \times (\mathrm{y_p}, \mathrm{y_{p+1}}]\right\}_{\mathrm{p=1,q=1}}^{\mathrm{P,Q}} \tag{S8}$$

Residuals are defined as:

$$r_i = z_i - \hat{z}(x_i, y_i) \forall z_i \in S \tag{S9}$$

To further enhance the robustness of outlier fitting, we adopt the Tukey loss function(Beaton and Tukey, 1974; Belagiannis et al., 2015), which suppresses the influence of mild outliers without compromising overall fitting performance. This improves the robustness of terrain normalization:

$$\mathcal{L}(r_i) = \begin{cases} \dfrac{\delta^2}{6}\left(1 - \left(1 - \dfrac{{r_i}^2}{\delta^2}\right)^3\right), |r_i| \le \delta \\ \dfrac{\delta^2}{6}, |r_i| > \delta \end{cases} \tag{S10}$$

To prevent degeneration of the covariance matrix and improve model stability, a regularization term is added to the final loss(Grave et al., 2011). Consequently, the optimization objective for the fitting stage is summarized as:

$$\arg \min_{\Theta} \sum_{\mathrm{i=1}}^{\mathrm{P\times Q}} \mathcal{L}(r_i) + \lambda \sum_{\mathrm{k=1}}^{\mathrm{K}} \mathrm{Tr}(\Sigma_k^{-1}) \tag{S11}$$

Where the model parameters are defined as:

$$\Theta = \{(\omega_k, A_k, \vec{\mu}_k, \Sigma_k)\}_{\mathrm{k=1}}^{\mathrm{K}} \tag{S12}$$

Comment 17: *Section 1.2.4: After reading this section, it was not clear to me which existing metrics you used. I would recommend adding a table here for those metrics, possibly with additional explanations, typical applications of the metric, references, etc.*

Response: Thank you for this helpful suggestion. We agree that the conventional VSC metrics used for comparison were not summarized clearly enough in the original manuscript. To improve clarity, we have added a new paragraph in the **supplymentary material** summarizing all existing LiDAR-derived VSC metrics used in this study, including their structural dimension, calculation logic, ecological interpretation, typical applications, and key references.

Specifically, the comparison included five conventional metrics: mean vegetation height, canopy cover, foliage height diversity (FHD), canopy rugosity, and canopy entropy. These metrics were selected because they represent different dimensions of vegetation structure, including vertical development, horizontal occupancy, vertical heterogeneity, canopy-surface roughness, and integrated three-dimensional structural complexity. These texts will help readers understand why these metrics were selected and how they differ from the proposed VSRE index.

Revised text and figures:

Description of conventional LiDAR-derived vegetation structural metrics used for comparison with VSRE

To evaluate whether VSRE captures vegetation structural complexity beyond existing LiDAR-derived metrics, we compared it with five representative structural metrics that have been widely used in forest and vegetation-structure studies. These metrics were selected because they describe different and complementary dimensions of vegetation structure, including vertical development, horizontal occupancy, vertical heterogeneity, canopy-surface roughness, and integrated three-dimensional occupancy.

- Mean vegetation height was used as a simple descriptor of vertical vegetation development. It was calculated as the mean height of all terrain-normalized LiDAR returns within each sample. This metric provides a direct estimate of the average vertical position of vegetation elements and has been widely used in studies of canopy height, biomass, productivity, and habitat structure.
- Canopy cover was used to represent horizontal vegetation occupancy. In this study, canopy cover was calculated as the proportion of LiDAR returns above a height threshold of 0.2 m. This metric reflects the degree to which vegetation elements occupy the horizontal ground area and is commonly used in vegetation-cover mapping, canopy-closure assessment, and habitat-structure studies (Atkins et al., 2018).
- Foliage height diversity was used to quantify vertical structural heterogeneity. It is based on the distribution of LiDAR returns among vertical height layers and is calculated using a Shannon diversity formulation. In this study, point heights were grouped into 0.5 m vertical layers before calculating the proportional occupancy of each layer. Foliage height diversity has been widely used to characterize vertical habitat complexity and canopy stratification (Macarthur and Macarthur, 1961).
- Canopy rugosity was used to describe canopy-surface complexity. It was calculated from the canopy height model generated from terrain-normalized LiDAR point clouds and reflects the degree of spatial variation in canopy height. Higher canopy rugosity generally indicates a more irregular canopy surface and has been used to characterize forest stand development, canopy roughness, and habitat heterogeneity (Parker and Russ, 2004).

- Canopy entropy was used as an integrated entropy-based descriptor of three-dimensional vegetation occupancy. This metric quantifies the uncertainty or evenness of point-cloud occupancy within canopy space and has recently been used to describe forest canopy structural complexity and its links to ecosystem functions. Compared with height- or surface-based metrics, canopy entropy incorporates more information from the three-dimensional point-cloud distribution (Liu et al., 2022).

Together, these five conventional metrics provide a broad benchmark for evaluating VSRE across horizontal, vertical, surface-based, and integrated three-dimensional structural dimensions. In contrast to these metrics, VSRE was designed to quantify local configurational heterogeneity by comparing normalized voxel-based point-cloud distributions among local windows using relative entropy. Therefore, VSRE does not primarily measure global space filling or overall point-occupancy evenness, but instead evaluates how much local structural configurations differ from one another across a vegetation patch.

Comment 18: *Section 1.2.5: Here, it is not clear to me what your target variable is. What are the class labels you want to predict? What are the features you use? I would recommend a table here as well.*

Response: Thank you for raising this important point. We agree that the organization of this section in the original manuscript was confusing. In particular, the vegetation classification component and the VSRE spatial mapping component were described together, which made it unclear whether the modelling target was a vegetation class label or a continuous VSRE value.

We would like to clarify the reason for this organization in the submitted manuscript. At the time of submission, the vegetation classification dataset and its associated methodological paper had not yet been formally published. Because this vegetation classification product was used as auxiliary ecological background information for interpreting VSRE patterns, we included a relatively complete methodological description in the original manuscript to keep the workflow transparent and reproducible. During the review process, this independent companion study was published online. Therefore, in the revised manuscript, we have shortened this part substantially and now cite the corresponding publication instead of repeating the full technical workflow. This revision also avoids unnecessary overlap between the two papers and keeps the present manuscript focused on VSRE development, validation, and application.

We further clarify that vegetation classification was not the main modelling objective of this study. The vegetation class labels, including *Spartina* spp., *Phragmites australis*, *Scirpus* spp., *Suaeda* spp., mixed marsh, and mangrove communities, were used only for ecological interpretation of VSRE differences among major coastal wetland communities. In contrast, the national-scale VSRE mapping was a regression task. The target variable was the LiDAR-derived VSRE value calculated from 1,337 field LiDAR samples, and the predictor variables were the 64-dimensional AlphaEarth Foundation embeddings extracted at the corresponding sample locations. These predictors were used to train the MLP regression model and generate the wall-to-wall 10 m VSRE map of coastal China.

Following your suggestion, we have revised the manuscript to explicitly distinguish the auxiliary vegetation-type information from the VSRE regression task. Because the original section has now been shortened and the detailed classification workflow is cited from the published companion study, we did not add a dense table to the main text.

Instead, we added a concise clarification in the Methods section and moved additional details to the Supplementary Materials.

Comment 19: *L258-267: You repeat a statement on resampling here: "The results were resampled using triple convolution […]", "The results are resampled into various vegetation indices through cubic convolution …". Which one is right?n.*

Response: Thank you for pointing this out. We apologize for this inconsistency. The phrase "triple convolution" was a wording error, and the correct term should be "cubic convolution". In the submitted manuscript, this statement was also repeated unnecessarily in the description of the vegetation-index preprocessing workflow.

In the revised manuscript, we have removed the duplicated sentence and corrected the terminology. Because the vegetation-index preprocessing and vegetation-classification workflow are no longer described in detail in the main text and are now mainly referred to through the published companion study, we have also shortened this part to avoid distracting from the main VSRE workflow. Where a resampling method needs to be mentioned, we now consistently use "cubic convolution".

Comment 20: *The Introduction and Section 1.2.3 should include a better high-level explanation of the index (cf. 1.3.1 in the results)*

Response: Thank you for this helpful suggestion. We agree that the conceptual explanation of VSRE should appear earlier in the manuscript, rather than being introduced mainly in the Results section. In the revised manuscript, the original Section 1.2.3 has been reorganized, and the detailed VSRE development is now presented in Section 1.2.4. We therefore added a brief high-level explanation of VSRE at the end of the Introduction and a short conceptual summary at the beginning of Section 1.2.4, before the detailed mathematical formulation.

Specifically, we now clarify that VSRE treats local voxelized LiDAR point-cloud distributions as representations of local vegetation structural configurations and uses relative entropy to quantify how different these local configurations are from one another. Therefore, higher VSRE values indicate greater spatial configurational heterogeneity in three-dimensional vegetation structure. These additions help readers understand the ecological meaning of the index before the technical implementation is introduced.

Revised text and figures:

Revised main text 1:

Based on the concept of relative entropy (RE, also known as the Kullback–Leibler divergence) (Cover and Thomas, 1991), this study developed a LiDAR point-cloud-derived VSC index, termed vegetation structure relative entropy (VSRE), to characterize heterogeneity in three-dimensional spatial configuration. Conceptually, VSRE treats the voxelized point-cloud distribution within each local window as a representation of local vegetation structure. It then uses relative entropy to quantify the degree of difference among these local three-dimensional structural configurations. Using high-precision UAV LiDAR observations and annual vegetation biomass survey data from 18 subplots (60 m × 60 m) at the largest water-level-controlled field experimental site worldwide, located on Chongming Island, Shanghai, China (**Fig. 1**), we systematically tested VSRE and compared its performance with several conventional

VSC metrics widely used in terrestrial ecosystems. Specifically, we evaluated the effectiveness and robustness of these metrics in quantifying VSC across typical coastal wetland vegetation scenarios, continuous complexity gradients, and different point cloud densities. We then applied VSRE to a high-density LiDAR dataset from 1,337 coastal vegetation sites spanning China's 18,400 km coastline. We combined the results with corresponding 2022 vegetation-type data to characterize VSC variation across typical natural vegetation communities in coastal wetlands of China. Finally, using the Alpha Earth Foundation (AEF) dataset and a multilayer perceptron (MLP) model, we generated a seamless 10 m spatial map of VSRE along the coast of China with high predictive accuracy ($R^2 = 0.96$).

Revised main text 2:

In simple terms, VSRE quantifies vegetation structural complexity by asking whether different local parts of a vegetation patch have similar or different three-dimensional point-cloud configurations. If neighboring or local windows have similar voxelized point distributions, the vegetation structure is interpreted as more homogeneous and VSRE remains low. If local windows differ strongly in their vertical and horizontal point distributions, the vegetation patch contains greater configurational heterogeneity and VSRE increases.

Comment 21: *Fig. 4: I do not understand where the aspect and the "varying PCD" are contained in this figure. Please explain this better.*

Response: Thank you for pointing this out. We agree that our original description of "varying PCD" was not sufficiently clear. In this analysis, "varying PCD" does not mean that PCD was displayed as an additional axis in the figure. Instead, we intentionally pooled samples from all point-cloud-density levels into a single mixed-PCD dataset. This design was used to test whether each VSC metric can still distinguish low-, medium-, and high-complexity vegetation groups when the input LiDAR samples have inconsistent point cloud densities.

This mixed-PCD scenario is important because, in practical LiDAR applications, point cloud density often varies among samples or survey regions due to differences in flight height, scanning geometry, vegetation occlusion, and environmental conditions. A robust VSC metric should therefore maintain its discriminatory ability even when the dataset contains mixed point densities. In the revised manuscript, we have clarified this point in both the Results text and the figure caption.

Revised figure:

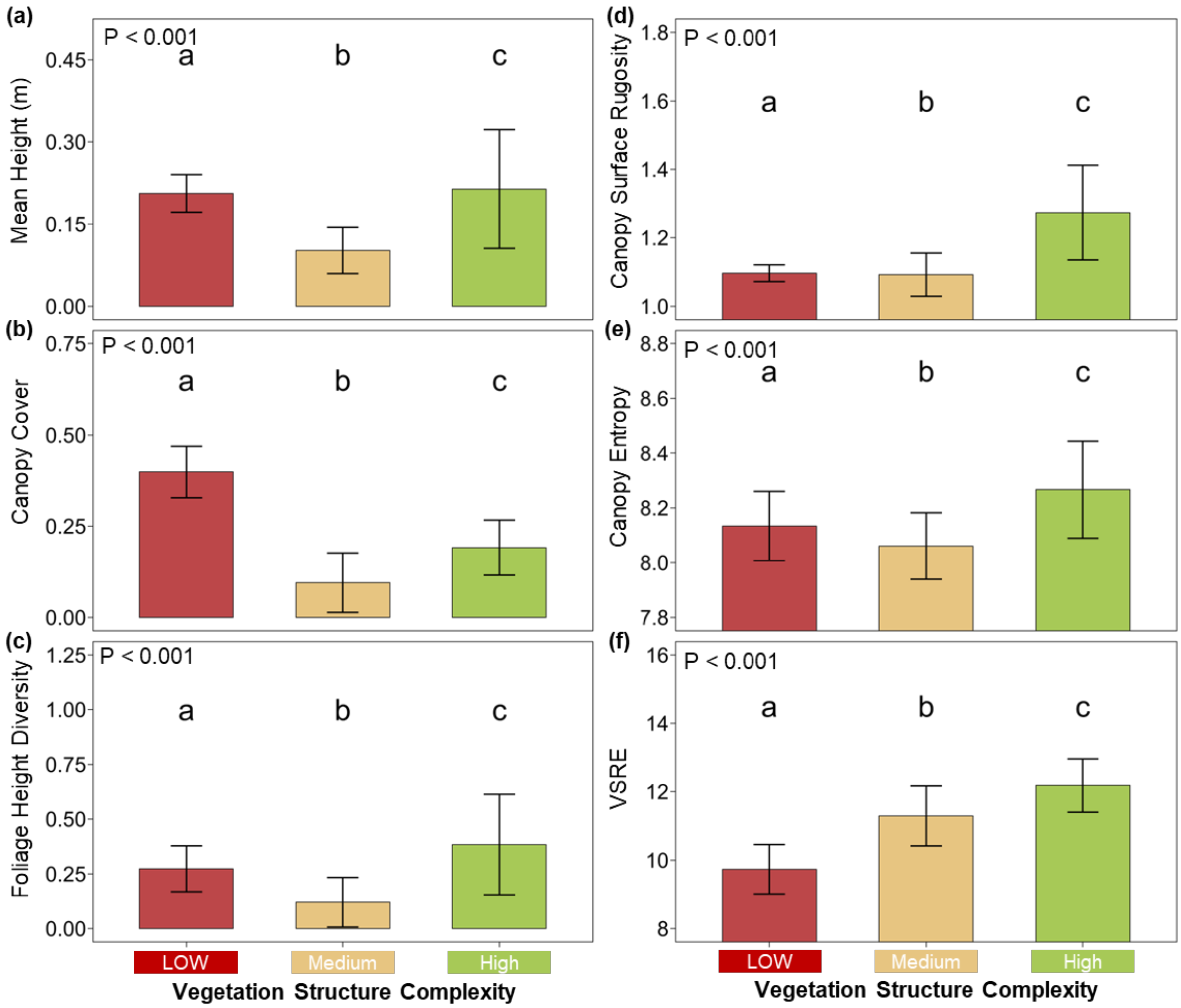

Fig. 5 | Robustness of VSRE and conventional VSC metrics under mixed point cloud densities. (a), mean vegetation height; **(b),** canopy cover; **(c)**, FHD (foliage height diversity); **(d)**, canopy rugosity; **(e)**, canopy surface entropy, and **(f)** VSRE. Bars indicate group means, and error bars denote the corresponding standard deviations. The Kruskal–Wallis test is applied to evaluate overall group differences, followed by Dunn's post hoc tests with Benjamin–Hochberg correction for pairwise comparisons. Different letters above boxes denote significant pairwise differences among groups. Groups with low, medium, and high VSC are color-coded in red, yellow, and green, respectively.

Comment 22: *Fig. 5: What does each circle represent in this figure? A UAV-LiDAR point cloud of a plot?*

Response: Thank you for this question. Yes, each circle represents one plot-level UAV-LiDAR sample used in the fixed-plot analysis. More specifically, each point corresponds to one secondary plot at a given point-cloud-density level, for which the corresponding VSC metric was calculated from the UAV-LiDAR point cloud and compared with the biomass-weighted Shannon index of that plot.

In the revised manuscript, this figure is now Fig. 6, and we have revised the caption to explicitly explain what each circle represents.

Revised figure:

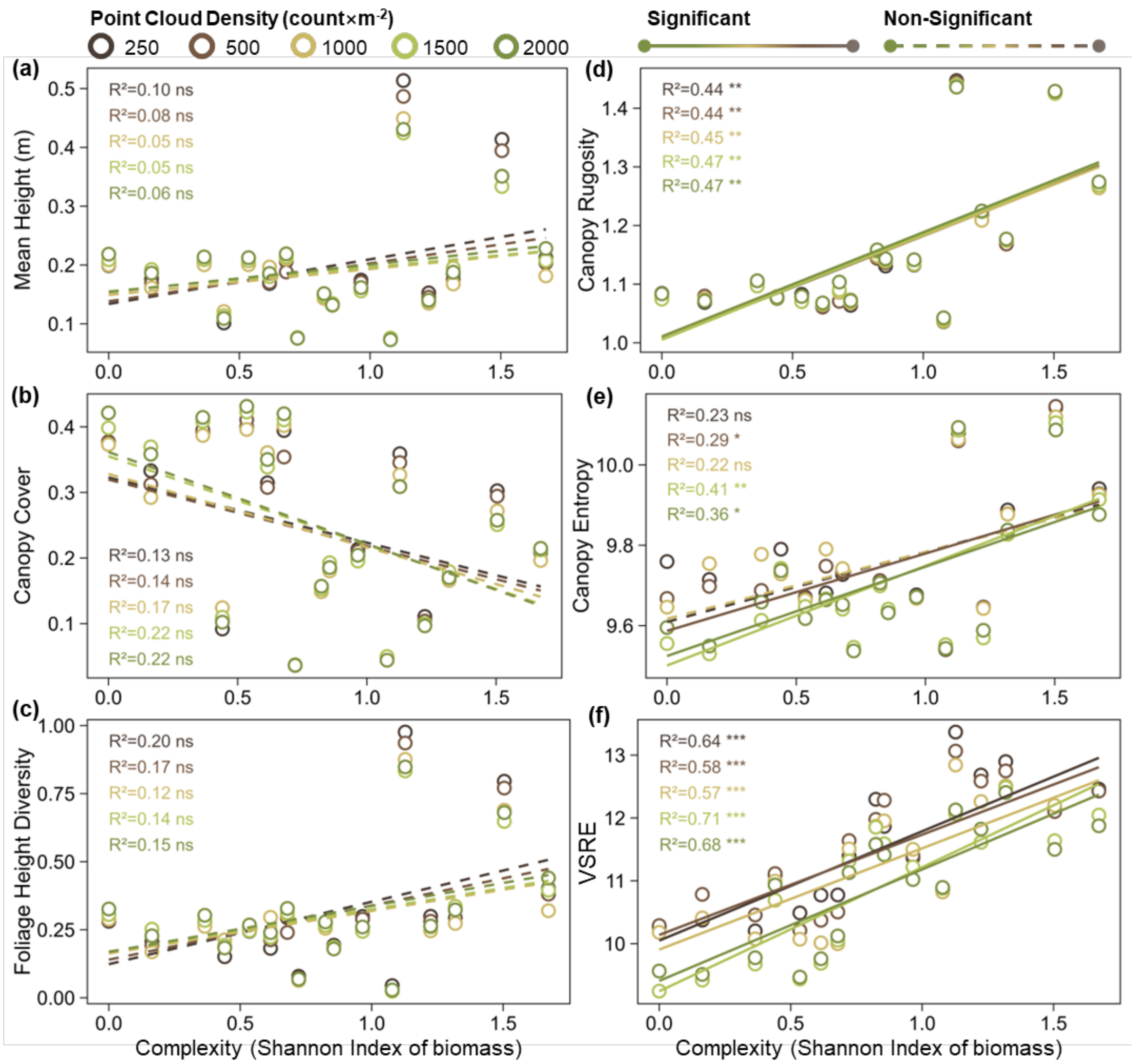

Fig. 6 | Linear trends in VSC indices with increasing quantitative complexity. (a), mean vegetation height; **(b),** canopy cover; **(c)**, FHD (foliage height diversity); **(d)**, canopy rugosity; **(e)**, canopy surface entropy, and **(f)** VSRE. Each circle represents one plot-level UAV-LiDAR sample from a secondary plot at a given PCD level. Low-to-high point cloud densities are represented by a color gradient from dark brown to dark green. Statistical test results and methods are annotated on the left side of each subplot.

Comment 23: *Guo et al. (2020) is cited in the text but missing in the references.*

Response: Thank you. We have cited the paper correctly.

Comment 24: *"L1 LiDAR sensor" -> DJI Zenmuse L1 LiDAR system?*

Response: Yes. We have revised the name of sensor to DJI Zenmuse L1 LiDAR system.

Comment 25: *Consistency: You sometimes used points/m2 and other times points m-2. You also sometimes used "formula" and sometimes "equation". Please make this consistent.*

Response: Thank you for carefully checking the consistency of the manuscript. We have standardized all point-cloud-density units as "points m^{-2}" throughout the manuscript. We have also standardized the terminology by using "equation" consistently when referring to mathematical expressions in the Methods and Supplementary Materials.

Comment 26: *VSRE is sometimes misspelled as VSER.*

Response: Thank you for pointing this out. We apologize for this typographical error. We have carefully checked the entire manuscript and Supplementary Materials and corrected all misspellings of "VSER" to "VSRE".

Comment 27: *Please check if the manuscript structure is according to the guidelines, e.g., should "Conclusions" be placed after "Data availability"?*

Response: Thank you for this helpful comment. We checked the ESSD submission guidelines and agree that the manuscript structure should be revised. We have reorganized the final part of the manuscript accordingly.

Comment 28: *It seems that your Supplementary Material would be better placed in the Appendix. Please read the "Submission" page (https://www.earth-system-science-data.net/submission.html) and evaluate whether "Appendix" or "Supplementary Material" is suitable for this material.*

Response: Thank you for this important suggestion. We carefully checked the ESSD submission guidelines and agree that most of our previous Supplementary Material is more suitable for the Appendix. According to the ESSD guidelines, supplementary material is mainly reserved for items that cannot reasonably be included in the main text or appendices, such as short videos, very large images, maps, or short computer codes. Normal-size figures and tables, as well as technical or theoretical developments that provide additional detail but would disrupt the flow of the main text, should instead be included as appendices.

Our previous Supplementary Material mainly contained normal-size supporting figures and tables, parameter-sensitivity analyses, model-comparison results, and technical details of terrain normalization. These materials provide useful methodological and technical support for the manuscript but are not separate research assets requiring an online supplement. Therefore, we have converted the previous Supplementary Material into Appendices and revised the corresponding citations throughout the manuscript.

Comment 29: *Some comments may be similar to those raised by Reviewer 1. In case you have already replied to them and revised the manuscript accordingly, you can of course simply refer to those replies. Please note that I did not review the Supplementary Material in more detail."*

Response: Thank you for this helpful note. We appreciate the reviewer's careful assessment and understand that some comments overlap with those raised by Reviewer 1. Where the same issues were raised by both reviewers, we have provided detailed responses in the relevant replies and have revised the manuscript accordingly.

Reference

Atkins, J. W., Bohrer, G., Fahey, R. T., Hardiman, B. S., Morin, T. H., Stovall, A. E., Zimmerman, N., and Gough, C. M.: Quantifying vegetation and canopy structural complexity from terrestrial Li DAR data using the forestr r package, Methods Ecol. Evol., 9, 2057-2066, 2018.

Beaton, A. E. and Tukey, J. W.: The fitting of power series, meaning polynomials, illustrated on band-spectroscopic data, Technometrics, 16, 147-185, 1974.

Belagiannis, V., Rupprecht, C., Carneiro, G., and Navab, N.: Robust optimization for deep regression, Proceedings of the IEEE international conference on computer vision, 2830-2838,

Cousins, S. H.: Species diversity measurement: choosing the right index, Trends Ecol. Evol., 6, 190-192, 1991.

Dalla Corte, A. P., Rex, F. E., Almeida, D. R. A. d., Sanquetta, C. R., Silva, C. A., Moura, M. M., Wilkinson, B., Zambrano, A. M. A., Cunha Neto, E. M. d., and Veras, H. F.: Measuring individual tree diameter and height using GatorEye High-Density UAV-Lidar in an integrated crop-livestock-forest system, Remote Sens., 12, 863, 2020.

Fischer, F. J., Maréchaux, I., and Chave, J.: Improving plant allometry by fusing forest models and remote sensing, New Phytol., 223, 1159-1165, 2019.

Grave, E., Obozinski, G. R., and Bach, F.: Trace lasso: a trace norm regularization for correlated designs, Advances in neural information processing systems, 24, 2011.

Jucker, T., Fischer, F. J., Chave, J., Coomes, D. A., Caspersen, J., Ali, A., Loubota Panzou, G. J., Feldpausch, T. R., Falster, D., and Usoltsev, V. A.: Tallo: A global tree allometry and crown architecture database, Global Change Biol., 28, 5254-5268, 2022.

Liu, X., Ma, Q., Wu, X., Hu, T., Liu, Z., Liu, L., Guo, Q., and Su, Y.: A novel entropy-based method to quantify forest canopy structural complexity from multiplatform lidar point clouds, Remote Sens. Environ., 282, 113280, 2022.

MacArthur, R. H. and MacArthur, J. W.: On bird species diversity, Ecology, 42, 594-598, 1961.

Morsdorf, F., Meier, E., Kötz, B., Itten, K. I., Dobbertin, M., and Allgöwer, B.: LIDAR-based geometric reconstruction of boreal type forest stands at single tree level for forest and wildland fire management, Remote Sens. Environ., 92, 353-362, 2004.

Parker, G. G. and Russ, M. E.: The canopy surface and stand development: assessing forest canopy structure and complexity with near-surface altimetry, For. Ecol. Manage., 189, 307-315, 2004.

Tian, N.: Growth models and profile equations for exotic tallow tree (Triadica sebifera) in coastal Mississippi, Mississippi State University2014.

Walker, S. M., Murray, L., and Tepe, T.: Allometric equation evaluation guidance document, Winrock International, USA, 75, 2016.

Wolfe, J. H.: Pattern clustering by multivariate mixture analysis, Multivar. Behav. Res., 5, 329-350, 1970.

Ye, N., Mason, E., Xu, C., and Morgenroth, J.: Estimating individual tree DBH and biomass of durable Eucalyptus using UAV LiDAR, Ecol. Inf., 89, 103169, 2025.